

## Conversion of Cellulose over Ni Loaded Mesoporous MSU-F Catalysts via Air Gasification

Young-Kwon Park,<sup>\*</sup> Kyung Sun Park, Seong-Soo Kim,<sup>†</sup> Sung Hoon Park,<sup>‡</sup>  
Sang-Chul Jung,<sup>‡</sup> Sang Chai Kim,<sup>§</sup> Jong-Ki Jeon,<sup>¶</sup> and Ki-Joon Jeon<sup>#,\*</sup>

Graduate School of Energy and Environmental System Engineering, University of Seoul, Seoul 130-743, Korea

<sup>\*</sup>E-mail: catalica@uos.ac.kr

<sup>†</sup>Korea Institute of Energy Research, Daejeon 305-343, Korea

<sup>‡</sup>Department of Environmental Engineering, Sunchon National University, Suncheon 540-950, Korea

<sup>§</sup>Department of Environmental Education, Mokpo National University, Muan 534-729, Korea

<sup>¶</sup>Department of Chemical Engineering, Kongju National University, Cheonan 330-717, Korea

<sup>#</sup>Department of Environmental Engineering, Inha University, Incheon 402-751, Korea. <sup>\*</sup>E-mail: kkjeon@inha.ac.kr

Received May 6, 2014, Accepted July 4, 2014

Catalytic gasification of cellulose was carried out in a U-type fixed reactor with Ni loaded MSU-F catalyst (Ni/MSU-F) and Ni loaded  $\gamma$ -Al<sub>2</sub>O<sub>3</sub> (Ni/ $\gamma$ -Al<sub>2</sub>O<sub>3</sub>). The characteristics of the catalysts were analyzed by using X-ray diffraction, H<sub>2</sub>-temperature programmed reduction, and Brunauer-Emmett-Teller analyses. The operation conditions of catalytic gasification reactions were 750 °C and 0.2 equivalence ratio. Air was used as gasification agent. Catalytic gasification characteristics, such as gas yield and gas composition (H<sub>2</sub>, CO, CO<sub>2</sub>, C<sub>1</sub>-C<sub>4</sub>), were measured and calculated. The gas yield of Ni/MSU-F was much higher than that of Ni/ $\gamma$ -Al<sub>2</sub>O<sub>3</sub>. Especially high amount of hydrogen was produced by Ni/MSU-F.

**Key Words :** H<sub>2</sub>, Cellulose, Air gasification, Ni/MSU-F

### Introduction

Biomass resources are plentiful in the world and can be easily commercialized than any other renewable resources. In spite of various biomass resources, two types of biomass-to-energy conversion technologies have been developed in the world. One is a biological pathway and the other is a thermochemical pathway.<sup>1-5</sup> Among the thermochemical conversion technologies, gasification converts biomass resources into syngas, which is composed mainly of hydrogen and carbon monoxide, at relatively high temperature.<sup>6-12</sup> The syngas produced from biomass gasification processes could be used to generate power by using a turbine or a gas engine or to make various chemicals and synthetic biofuels by using Fischer-Tropsch reaction. However tar, a byproduct of biomass gasification processes must be removed before the utilization of syngas.<sup>8,9,11,13,14</sup>

Tar, a mixture of poly-aromatic compounds with large molecular mass, causes the blockage of lines and results in the shutdown of plants. To reduce tar from biomass gasification processes, a filtration using a ceramic filter and a catalytic conversion process have been applied.<sup>15</sup> Especially the catalytic conversion process is more valuable because it can decompose tar into CO and H<sub>2</sub> and then increase the content of CO and H<sub>2</sub>. In the tar decomposition process Ni/ $\gamma$ -Al<sub>2</sub>O<sub>3</sub> is widely applied.<sup>13,16</sup> But the decline of activity due to carbon deposition is a critical problem of the Ni/ $\gamma$ -Al<sub>2</sub>O<sub>3</sub> catalyst. Various support materials have been developed to overcome the declining activity of catalysts and to enhance the activity of Ni. Since mesoporous materials among vari-

ous support materials have higher surface areas and have enough room to add metal components, catalysts with mesoporous support materials have outstanding activities in case of biomass conversion reactions. Therefore, mesoporous materials with Ni are expected to have good activity in biomass gasification. Though MSU-F support material among mesoporous support materials has not been used in biomass catalytic gasification, MSU-F is a promising support material because the high surface area and large pore size of MSU-F are enough to add Ni and make the diffusion of tar particles with large molecular size into the pores easier.

Generally, lignocellulosic biomass resources are composed of cellulose, hemicellulose, and lignin.<sup>17-19</sup> Especially, the weight fraction of cellulose is about 35-50 wt %. Therefore, the gasification reaction of cellulose might provide the basic data of biomass gasification reactions. The catalytic gasification characteristics have been studied by using steam as gasification agent. However, the catalytic gasification of cellulose with air as gasification agent was carried out using Ni loaded MSU-F (Ni/MSU-F) in this study for the first time. Also, the catalytic gasification experiments of cellulose with Ni loaded  $\gamma$ -Al<sub>2</sub>O<sub>3</sub> (Ni/ $\gamma$ -Al<sub>2</sub>O<sub>3</sub>) have also been conducted in this study to compare the catalytic activity of Ni/MSU-F with that of Ni/ $\gamma$ -Al<sub>2</sub>O<sub>3</sub>. In this study, we are aiming to test a Ni/MSU-F as a catalyst for attaining a higher gas yield (especially H<sub>2</sub>) than Ni/ $\gamma$ -Al<sub>2</sub>O<sub>3</sub>.

### Experimental

Cellulose was purchased from Sigma-Aldrich. Cellulose is

composed of 1.1% of moisture, 95.4% of volatile matters, 2.1% of fixed carbon, and 1.4 wt % of ash. The elemental analysis showed that it consisted of C (42.99 wt %), H (5.94 wt %), and O (51.07 wt %). For more detailed results of elemental and proximate analyses, one can refer to previous studies published.<sup>20,21</sup>

MSU-F and  $\gamma$ -Al<sub>2</sub>O<sub>3</sub> were purchased from Sigma-Aldrich.  $\gamma$ -Al<sub>2</sub>O<sub>3</sub> was impregnated with 5 wt % of Ni using the incipient wetness method. MSU was impregnated with 5 and 15 wt % of Ni using the incipient wetness method. The precursor of Ni was Ni(NO<sub>3</sub>)<sub>3</sub>·6H<sub>2</sub>O. Prepared catalysts were calcined at 650 °C for 3 h in muffle furnace.

The characteristics of the Ni-impregnated catalysts were examined. Specific surface area was measured using the Brunaur-Emmett-Teller (BET) method. X-ray diffraction (XRD) patterns were obtained at room temperature by a Rigaku D/MAX-III instrument equipped with a Cu K $\alpha$  X-ray source. Reducibility was evaluated by BELCAT using the H<sub>2</sub>-temperature-programmed reduction (TPR) method. For more detailed procedure of catalyst characterization, one can refer to a previous study published.<sup>16</sup> Conventional transmission electron microscopy (TEM) was also used to study the size of Ni particle and the degree of its dispersion over the catalyst. The TEM sample was prepared by depositing a drop of sample solution on a 3 nm thick amorphous carbon-coated TEM grid, which was air-dried prior to TEM characterization in JEM2100F.

Catalytic gasification was conducted at 750 °C in a U-type fixed reactor made of quartz. The volume, height, and inlet/outlet diameter were 50 mL, 160 mm, and 15 mm, respectively. Air was used as the gasifying agent and equivalence ratio (ER) of 0.2 was applied. The vapor-phase product was cooled in two condensers. The condenser temperature was controlled at -20 °C by a circulator for sufficient condensation of bio-oil. The product gas that passed the condensers was collected in a Teflon gas bag for further analysis. For catalytic gasification, two reactors were employed. Non-catalytic reaction took place in the first reactor, while the catalytic upgrading of product vapor occurred in the second reactor that contained a catalyst layer. The mass ratio between the catalyst and biomass was 1:10 in the second method.

## Results and Discussion

The surface areas of  $\gamma$ -Al<sub>2</sub>O<sub>3</sub> and MSU-F used as catalyst support materials were 113 m<sup>2</sup>/g and 602 m<sup>2</sup>/g, respectively. The pore size of MSU-F was about 11.6 nm. The surface areas of MSU-F and  $\gamma$ -Al<sub>2</sub>O<sub>3</sub> decreased due to the addition of Ni. The surface area of Ni/ $\gamma$ -Al<sub>2</sub>O<sub>3</sub> containing 15 wt % Ni was 45 m<sup>2</sup>/g, whereas the surface area of Ni/MSU-F containing 5 wt % and 15 wt % Ni was 450 m<sup>2</sup>/g and 385 m<sup>2</sup>/g, respectively.

The XRD patterns of Ni/MSU-F and Ni/ $\gamma$ -Al<sub>2</sub>O<sub>3</sub> are shown in Figure 1. Ni peaks were observed at 37, 43, 64° which were assigned for NiO (101), NiO (012) and NiO (110), respectively.<sup>22</sup> 15 wt % Ni/MSU-F showed higher peak

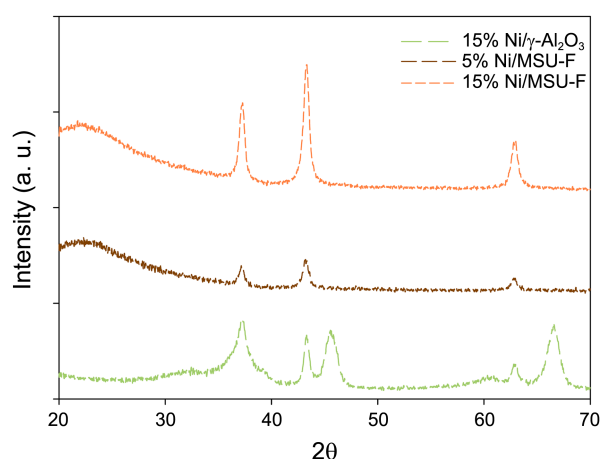


Figure 1. XRD patterns of Ni based catalysts.

intensity than 15 wt % Ni/ $\gamma$ -Al<sub>2</sub>O<sub>3</sub>, indicating that the Ni particles in MSU-F are larger than those in  $\gamma$ -Al<sub>2</sub>O<sub>3</sub>. The mean Ni crystallite size calculated using Scherrer equation was 51.2 nm and 35.8 nm for 15 wt % Ni/MSU-F and 15 wt % Ni/ $\gamma$ -Al<sub>2</sub>O<sub>3</sub>, respectively. Ni is known to be dispersed more evenly on acidic support materials than on non-acidic ones.<sup>23</sup> In this study, too, an acidic support  $\gamma$ -Al<sub>2</sub>O<sub>3</sub> led to a much better dispersion of Ni (smaller Ni crystallite particles), despite its much smaller surface area, than MSU-F. The mean Ni crystallite size of 5 wt % Ni/MSU-F was 28.4 nm, which is also much larger than the mean pore size of MSU-F (11.6 nm), implying that a considerable amount of Ni existed outside the pores.

Figure 2 shows the TEM images of Ni based catalysts. The average Ni particle sizes of 15 wt % Ni/MSU-F and 15 wt % Ni/ $\gamma$ -Al<sub>2</sub>O<sub>3</sub> were 45.2 nm and 20.9 nm, respectively, which were quite close to the results of XRD.

The TPR results of Ni-added catalysts are shown in Figure 3. The reduction peak of 15 wt % Ni/MSU-F appeared at approximately 420 °C and 620 °C, representing Ni particles existing on external surface and inside the pores, respectively. The 420 °C peak showed much larger peak area, indicating that most Ni particles existed on the external surface, which is in good agreement with the XRD result. In the case of 5 wt % Ni/MSU-F, too, more Ni particles existed on the external surface than inside the pores. On the other hand, 15 wt % Ni/ $\gamma$ -Al<sub>2</sub>O<sub>3</sub> exhibited a weak shoulder peak at 410 °C

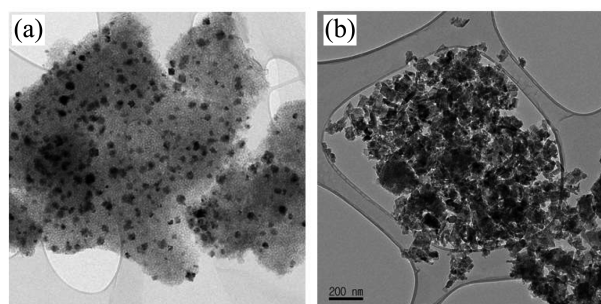


Figure 2. TEM images of Ni based catalysts (a) Ni/MSU-F (b) Ni/ $\gamma$ -Al<sub>2</sub>O<sub>3</sub>.

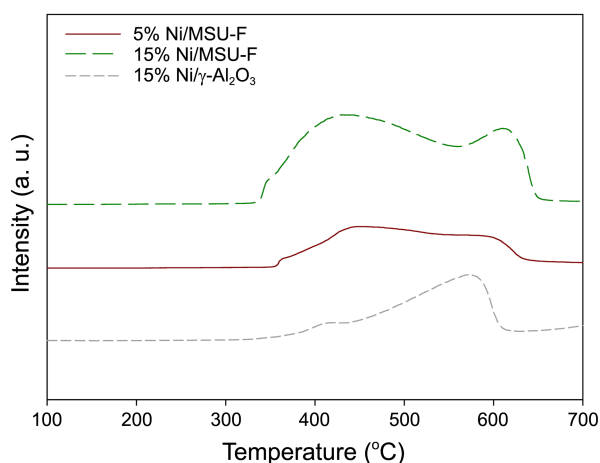


Figure 3. TPR results of Ni based catalysts.

and a main peak at 580 °C, suggesting that Ni particles existed mostly inside the pores of  $\gamma$ -Al<sub>2</sub>O<sub>3</sub>. Also, Wu *et al.*<sup>24</sup> ascribed the first reduction peak at lower temperature to large NiO crystals which were formed outside the pores of Ni/MCM-41 catalysts. Meanwhile, the second reduction peak at high temperature was attributed to small NiO particles inside the pores of the Ni/MCM-41 catalysts. Their suggestion matches our results well. Meanwhile, the high temperature peak implying strong interaction between Ni oxides and MSU-F may be originated from the reduction of nickel silicate,<sup>25</sup> whereas the low temperature peak may imply weak interaction between Ni oxides and MSU-F. TPR peaks intensity, XRD peak intensity, and TEM results indicate that most NiO may exist on the outside surface of MSU-F as weak interacting NiO species.

The total TPR curve area of 15 wt % Ni/ $\gamma$ -Al<sub>2</sub>O<sub>3</sub> was much smaller than that of 15 wt % Ni/MSU-F and similar with that of 5 wt % Ni/MSU-F. This is attributed to the formation of NiAl<sub>2</sub>O<sub>4</sub>, which is resistant to gasification, by strong metal-support interaction between Ni and alumina support in Ni/ $\gamma$ -Al<sub>2</sub>O<sub>3</sub>.<sup>23,26</sup> The presence of the main TPR reduction curve at low temperature and large curve area of Ni/MSU-F suggests that the reducibility of Ni/MSU-F is stronger than that of Ni/ $\gamma$ -Al<sub>2</sub>O<sub>3</sub>.

The catalytic gasification results of cellulose with air as the gasification agent are shown in Figure 4. The gasification yields of gas, oil, and char without catalyst were 34 wt %, 61 wt %, and 5 wt %, respectively. In the case of catalytic gasification, the gas content increased to 56 wt % and oil content decreased to 29 wt %. Especially, the gas yield obtained with Ni/MSU-F was higher than that with Ni/ $\gamma$ -Al<sub>2</sub>O<sub>3</sub>. The gas yield of 5 wt % Ni/MSU-F was higher than that of 15 wt % Ni/ $\gamma$ -Al<sub>2</sub>O<sub>3</sub>. It means that MSU-F support material might be advantageous for gasification reaction compared with  $\gamma$ -Al<sub>2</sub>O<sub>3</sub> support material. Because the reducing ability of Ni/MSU-F is superior to that of Ni/ $\gamma$ -Al<sub>2</sub>O<sub>3</sub> as shown in Figure 3, the gasification reaction of Ni/MSU-F might be more active than that of Ni/ $\gamma$ -Al<sub>2</sub>O<sub>3</sub> and the gas yield of Ni/MSU-F was higher than that of Ni/ $\gamma$ -Al<sub>2</sub>O<sub>3</sub>. Also the gas yield increased with increasing Ni content from 5

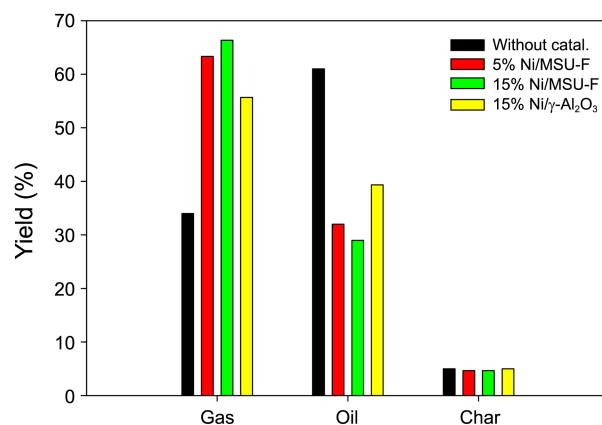


Figure 4. Product yields of air gasification of cellulose with ER = 0.2.

wt % to 15 wt %. However, even with three times higher Ni content, the gas yield obtained with 15 wt % Ni/MSU-F was only slightly higher than that obtained with 5 wt % Ni/MSU-F, probably because the increased amount of Ni resulted in poor dispersion of Ni existing on the external surface of MSU. Further investigation on the optimal amount of Ni to be impregnated will be required.

Syngas components from gasification experiments with and without catalysts are shown in Figure 5. Major products of the air gasification were CO and CO<sub>2</sub>. However, the hydrogen concentrations increased in the case of the catalytic gasification. Especially, the hydrogen selectivity of Ni/MSU catalyst was higher than that of Ni/ $\gamma$ -Al<sub>2</sub>O<sub>3</sub> catalyst. For example, hydrogen content obtained with 5 wt % Ni/MSU-F was higher than that with 15 wt % Ni/ $\gamma$ -Al<sub>2</sub>O<sub>3</sub>. Similar to the results of Ni/CeO<sub>2</sub>-ZrO<sub>2</sub>,<sup>16</sup> Ni/MSU-F catalysts of which the reduction capability was superior might promote biomass gasification reaction. Also, hydrogen content increased and the content of CO and CO<sub>2</sub> decreased with increasing Ni content from 5 wt % to 15 wt %.

Li *et al.*<sup>27</sup> suggested that there were 7 different reactions in the case of catalytic gasification over Ni based catalysts. As shown in Figure 4, catalytic gasification over Ni/MSU-F and Ni/ $\gamma$ -Al<sub>2</sub>O<sub>3</sub> catalysts produced lots of hydrogen compared

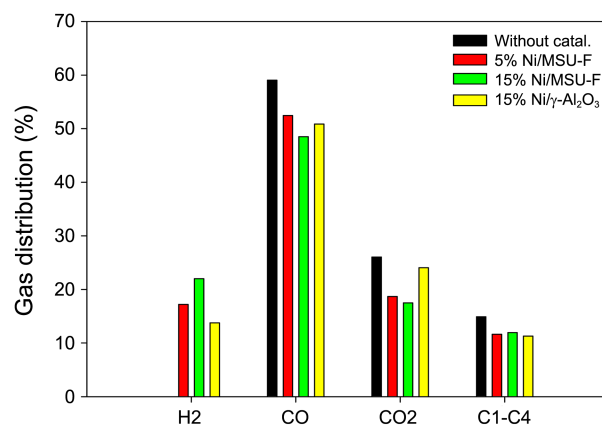
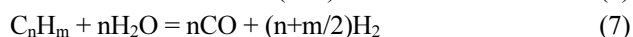
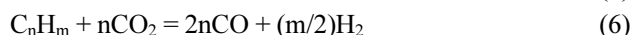


Figure 5. Gas composition after catalytic air gasification of cellulose at ER = 0.2.

with non-catalytic gasification reaction. It means that reactions (4)–(7), which are related with hydrogen production, might actively occur during the biomass catalytic gasification. Especially, the comparison of the H<sub>2</sub> yields and oil yields obtained from the catalytic gasification reactions suggested that Ni/MSU catalysts might promote tar decomposition reactions (6, 7) better than Ni/γ-Al<sub>2</sub>O<sub>3</sub> catalysts. However, researches on the detailed mechanism by using model compounds such as naphthalene are needed to confirm the tar decomposition reactions by Ni based catalysts.



### Conclusion

Catalytic gasification experiments were carried out using a U-type fixed bed reactor with air as the gasification agent. Compared with non-catalytic gasification, catalytic gasification of cellulose increased syngas yield and decreased oil yield due to vivid tar decomposition by the catalysts. Especially, catalytic gasification increased H<sub>2</sub> concentration in syngas. Also, Ni/MSU-F showed higher gasification ability than Ni/γ-Al<sub>2</sub>O<sub>3</sub>. This may be attributed to the fact reducibility of Ni increased more by MSU-F than by γ-Al<sub>2</sub>O<sub>3</sub>.

**Acknowledgments.** This work was supported by the research program of Korea Institute of Energy Research (Project No. B3-2426). This work was also supported by INHA UNIVERSITY Research Grant (INHA-49291-1).

### References

- Zhou, C. H.; Xia, X.; Lin, C. X.; Tong, D. S.; Beltrami, J. *Chem. Soc. Rev.* **2011**, *17*, 549.
- Pidtasang, B.; Udomsap, P.; Sukkasi, S.; Chollacoop, N.; Pattiya, A. *J. Ind. Eng. Chem.* **2013**, *19*, 1851.
- Bulushev, D. A.; Ross, J. R. H. *Catal. Today* **2011**, *171*, 1.
- Lee, H. J.; Lim, W. S.; Lee, J. W. *J. Ind. Eng. Chem.* **2013**, *19*, 2010.
- Ko, C. H.; Park, S. H.; Jeon, J. K.; Suh, D. J.; Jeong, K. E.; Park, Y. K. *Korean J. Chem. Eng.* **2012**, *29*, 1657.
- Lasa, D.; Salas, E.; Mazumder, J.; Lucky, R. *Chem. Rev.* **2011**, *111*, 5404.
- Xu, C.; Donald, J.; Byambajav, E.; Ohtsuka, Y. *Fuel* **2010**, *89*, 1784.
- Palma, C. F. *Appl. Energy* **2013**, *111*, 129.
- Shen, Y.; Yoshikawa, K. *Renew. Sustain. Energy Rev.* **2013**, *21*, 371.
- Li, F.; Huagn, J.; Fang, Y.; Wang, Y. *Korean J. Chem. Eng.* **2013**, *30*, 2013.
- Kim, Y. K.; Park, J. I.; Jung, D.; Miyawaki, J.; Yoon, S. H.; Mochida, I. *J. Ind. Eng. Chem.* **2014**, *20*, 9.
- Park, I. H.; Park, Y. K.; Lee, Y. M.; Bae, W.; Kwak, Y. H.; Cheon, K. H.; Park, S. H. *Appl. Chem. Eng.* **2011**, *22*, 286.
- Park, H. J.; Park, S. H.; Sohn, J. M.; Park, J.; Jeon, J. K.; Kim, S. S.; Park, Y. K. *Bioresour. Technol.* **2010**, *101*, S101.
- Xue, Q.; Liu, Y. *J. Ind. Eng. Chem.* **2012**, *18*, 1741.
- Nacken, M.; Heidenreigh, S.; Verpoort, F.; Baron, G. V. *Appl. Catal. B: Environ.* **2012**, *125*, 111.
- Kim, S. S.; Kim, J. W.; Park, S. H.; Jung, S. H.; Jeon, J. K.; Ryu, C.; Park, Y. K. *Bull. Korean Chem. Soc.* **2013**, *34*, 3387.
- Jeon, M. J.; Jeon, J. K.; Suh, D. J.; Park, S. H.; Sa, Y. J.; Joo, S. H.; Park, Y. K. *Catal. Today* **2013**, *204*, 170.
- Lee, H. W.; Park, S. H.; Jeon, J. K.; Ryoo, R.; Kim, W.; Suh, D. J.; Park, Y. K. *Catal. Today* **2014**, *232*, 119.
- Kim, T. H.; Jeon, Y. J.; Oh, K. K.; Kim, T. H. *Korean J. Chem. Eng.* **2013**, *30*, 1339.
- Park, Y. K.; Jun, B. R.; Park, S. H.; Jeon, J. K.; Lee, S. H.; Kim, S. S.; Jeong, K. E. *J. Nanosci. Nanotechnol.* **2014**, *14*, 5120.
- Jun, B. R.; Jeong, K. E.; Joo, S. H.; Sa, Y. J.; Park, S. H.; Jeon, J. K.; Park, Y. K. *J. Nanosci. Nanotechnol.* **2013**, *13*, 7794.
- Cho, Y. S.; Park, J. C.; Lee, B.; Kim, Y. H.; Yi, J. *Catal. Lett.* **2002**, *81*, 89.
- Yang, Y.; Ochoa-Hernández, C.; de la Peña O'Shea, V. A.; Pizarro, P.; Coronado, J. M.; Serrano, D. P. *Appl. Catal. B: Environ.* **2014**, *145*, 91.
- Wu, C.; Wang, L.; Williams, P. T.; Shi, J.; Huang, J. *Appl. Catal. B: Environ.* **2011**, *108-109*, 6.
- Wang, Y.; Zhu, A.; Zhang, Y.; Au, C. T.; Yang, X.; Shi, C. *Appl. Catal. B: Environ.* **2008**, *81*, 141.
- Li, G.; Hu, L.; Hill, J. M. *Appl. Catal. A: Gen.* **2006**, *301*, 16.
- Li, J.; Liu, J.; Liao, S.; Yan, R. *Int. J. Hydrogen Energy* **2010**, *35*, 739.